Xijun Hua
School of Mechanical Engineering,
Jiangsu University,
Zhenjiang, Jiangsu 212013, China

Jianguo Sun[1]
School of Mechanical Engineering,
Jiangsu University,
Zhenjiang, Jiangsu 212013, China
e-mail: 15751010096@163.com

Peiyun Zhang
School of Mechanical Engineering,
Jiangsu University,
Zhenjiang, Jiangsu 212013, China

Kai Liu
School of Mechanical Engineering,
Jiangsu University,
Zhenjiang, Jiangsu 212013, China

Rong Wang
School of Mechanical Engineering,
Jiangsu University,
Zhenjiang, Jiangsu 212013, China

Jinghu Ji
School of Mechanical Engineering,
Jiangsu University,
Zhenjiang, Jiangsu 212013, China

Yonghong Fu
School of Mechanical Engineering,
Jiangsu University,
Zhenjiang, Jiangsu 212013, China

Tribological Properties of Laser Microtextured Surface Bonded With Composite Solid Lubricant at High Temperature

A combination technology of the solid lubricant and the laser surface texturing (LST) can significantly improve the tribological properties of friction pairs. The plate sample was textured by fiber laser and composite lubricant of polyimide (PI) and molybdenum disulfide (MoS_2) powders were filled in the microdimples. Sliding friction performances of micron-sized composite lubricant and nano-sized composite lubricant were investigated by ring-plate tribometer at temperatures ranging from room temperature (RT) to 400 °C. On the one hand, the results of the micron-sized composite lubricant show that the friction coefficient of the textured surface filled with composite lubricant (TS) exhibits the lowest level and the highest stability compared to a textured surface without solid lubrication, smooth surface without lubrication, smooth surface burnished with a layer of composite solid lubricant. The better dimple density range is 35–46%. The friction coefficients of the sample surface filled with micron-composite solid lubricant with the texture density of 35% are maintained at a low level (about 0.1) at temperatures ranging from RT to 300 °C. On the other hand, the results of the nano-sized composite lubricant show that these friction properties are better than those of MoS_2-PI micron-sized composite. The friction coefficients of MoS_2-PI-CNTs nano-sized composite solid lubricant are lower than those of the MoS_2-PI composite lubricant at temperatures ranging from RT to 400 °C. In addition, the possible mechanisms involving the synergetic effect of the surface texture and the solid lubricant are discussed in the present work.
[DOI: 10.1115/1.4032522]

Keywords: laser surface texturing, composite solid lubricant, self-lubrication mechanism, sliding friction

1 Introduction

Surface texturing has a remarkable influence on the tribological properties of friction pair surfaces [1–3]. It can be produced by Laser processing technology [4], reactive ion etching technology [5], photochemical machining technology [6], machining technology, and so on. Up to now, LST, the most widely used technology among many practical surface texturing methods has been successfully applied to mechanical seals [7], gas seals [8], thrust bearings [9], journal bearings [10], piston rings [11], and so on. Solid lubricants meet some important and critical tribological needs due to the facts that they are chemically stable, preferably adhere strongly, can provide low and constant friction, and can be used in severe conditions [12]. In recent years, enormous efforts combining LST with incorporation of solid lubricant into microreservoirs have been made to refine the tribological properties [13–17]. The fundamental benefits of LST are to trap wear particles and to make reservoirs for lubricants capable of feeding the lubricant directly between the two contacting surfaces [13]. By now, the solid lubricant films are mostly designed by using the methods of burnishing, sputter deposition, and so on. However, these films have some shortcomings such as low adherence with substrate especially for burnishing coating and the low denseness of filler (solid lubricant) in the dimples. To improve the adhesion between the ground steel and the film, Rapoport et al. [18] adopted a method where a sublayer of nanoparticles (CdZnSe) was burnished on a virgin steel surface and then MoS_2 particles were burnished on the surface of CdZnSe sublayer, and the results showed that the adhesion and wear life of the solid lubricant films were increased. However, deposition procedures are complex and materials processed are strictly required in the methods. An effective method was adopted by Hu et al. [19] that MoS_2 solid lubricant coating was fabricated by a combination technology of laser texturing and hot-pressing, and the result showed that the wear life of the hot pressed coating was 15 times higher than that of the coating fabricated by burnishing. Though the method was simple and the adherence with substrate had been improved, the large thickness of the lubricant film fabricated by hot-pressing made the assembly difficult for some high precision friction pair, and the adherence with substrate might be further improved if some adhesive was added. Therefore, it is urgent to explore a method where the lubricant is fully filled in the microdimples and has a strong adherence with substrate without changing the thickness of the friction pair.

Lubrication over a wide temperature range has been a challenge in recent decades, which has aroused interest among many researchers [20–22]. In order to meet the special requirements at high temperature, composite lubricant or duplex-treatment process is usually employed. The lubricating effects of these combinations are good over a wide temperature range because the lubricants complement each other. The friction coefficients of the textured silver-containing nickel-based alloy smeared with MoS_2 were reduced at temperatures ranging from RT to 400 °C [23]. Li et al. [24] infiltrated Mo and filled MoS_2 on the textured stainless steel

[1]Corresponding author.

Contributed by the Tribology Division of ASME for publication in the Journal of Tribology. Manuscript received July 14, 2015; final manuscript received January 15, 2016; published online April 25, 2016. Assoc. Editor: Daniel Nélias.

surface by the double glow plasma infiltration technology. As a result, the friction coefficient and the wear rate decreased, compared to the only textured one. Oksanen et al. [25] made a ta-C coating on the textured stainless steel and then burnished WS_2 addition. The results showed that WS_2 addition increased remarkably the wear life of ta-C at 250 °C and low friction coefficient values (0.01–0.02) were achieved.

Appropriate proportions of adhesive and solid lubricant as well as operating condition have obvious influence on the friction coefficient [26,27]. PI has outstanding heat resistance and mechanical properties [28].The friction coefficient of the composite of PI modified by MoS_2 decreased with the increase of load, which showed better friction properties [29]. The PI/MoS_2 intercalation composite material synthesized, and as additive in lithium grease had good friction reduction and antiwear effect on steel–steel friction pair [30]. The previous studies on the friction characteristics of laser microtexturing surface filled with solid lubrication often utilize molybdenum disulfide or graphite as lubricant [31] and the particles are often confined to micron-sized. However, few researches have been carried out on the tribological properties of laser microtexturing surface bonded with micron-sized composite solid lubrication and nano-sized composite solid lubrication at high temperature. In addition, although the MoS_2-PI composite solid lubricant has low friction coefficient, the hardness and bearing capacity of MoS_2-PI composite solid lubricant film are relatively low, and thus the solid lubricating film is easily damaged. However, carbon nanotubes (CNTs) are often used as the additive of solid lubricating material, in order to improve the friction reduction and antiwear properties of the solid lubricants because they have fine mechanical properties, favorable high temperature adaptability, and good lubricating property [32–34].

The aim of this work is to study the elevated temperature friction and wear performance of sliding contact surfaces and to explore the lubrication mechanism of the textured surface filled with micron-sized MoS_2 and nano-sized MoS_2, PI and CNTs, which provides a theoretical reference for the research and development of high temperature composite solid lubricating material. In this paper, the microdimple morphology was machined on the surface of Cr4Mo4V high temperature bearing steel by LST technology.

2 Test Equipment and Research Methods

2.1 Raw Material. Micron-sized Molybdenum disulfide: produced in Shanghai Shenyu Industry & Trade Co., Ltd., purity of 99.5%, particle size of 0.5 μm; SKPI-MS10 type PI powder: Changzhou City Branch Special Polymer Materials Co. ltd. Nano-sized Molybdenum disulfide: produced in Nanjing Aipurui Composite Material Co. Ltd, purity of 99.5%, particle size of 40 nm; CNTs: produced in Qinhuangdao City Taijihuan Nanometer Co., Ltd, the length of 3–12 μm, diameter of 3.5–12.9 nm.

2.2 The Sample Processing and Preparation. The materials of the upper and lower samples with hardness of 67 HRC and roughness (Ra) of 0.1 μm are Cr4Mo4V high temperature bearing steel, as shown in Fig. 1. The diagram of friction pair is shown in Fig. 2. The LST was carried out on the lower sample surface using the YLP-HP-1-100-100-100 fiber laser (wavelength 1064 nm, the pulse width 100 ns, laser power 50 W, frequency 50,000 Hz). And the upper sample is untextured. Dimples with diameters ranging from 79 to 81 μm and depths of 15–17 μm (Fig. 1) were fabricated on the lower surface in the form of formula arrays according to the previous research on laser processing test in our research group. The texture density of Figs. 3 and 4 is 23%. The textured sample surface was polished by the metallographic sample polishing machine.

The molybdenum disulfide and PI were well-distributed according to the 80 wt.% MoS_2 +20 wt.% PI. In order to refine the tribological performance of the microtextured surface filled with solid lubricant, 6 wt.% CNTs were supplemented in MoS_2-PI composite solid lubricant, and the composite powders were smeared evenly on the lower surface of the sample. The molding processes of pressure-maintaining and pressure-heat were adopted to prepare sample blank. The prepared samples were processed into friction and wear test specimens after polishing treatment with the W_5 blank gold paper, as shown in Fig. 5. The microdimple can be used as the storage of lubricants. The effect of storage of solid lubricant varied with the dimple density, which can be defined as $Td = \pi\ (D^2/4L^2) \times 100\%$, where L is the distance between dimples and D is the diameter of dimple. The diameter of microdimples is 80 μm, and the texture density is 12%, 23%, 35%, 46%, and 58%.

2.3 Test Equipment and Method. The friction and wear properties of the samples were evaluated by the MMU-10 G high temperature friction and wear testing machine (see Fig. 6). The lower sample kept still while the upper sample rotated. The contact mode of the ring surface and the lower textured surface was surface contact. The whole system was surrounded by an electrical furnace, in which the environment temperature ranges from RT to 400 °C. The whole samples are shown in Table 1. The phase composition of the solid material filled in the textured sample was analyzed by X-ray diffraction (XRD) after the wear test in the temperature range of RT to 400 °C. The morphology of the sample surface was observed by three-dimensional morphology analyzer (Wyko-NT1100, Veeco, Tucson, AZ), and scanning electron microscopy (JSM-7001 F, JOEL, Beijing, China) attached with energy-dispersive spectrum (EDS). The experimental conditions are the load of 100–500 N with contact pressure of 0.46–2.31 MPa, speed of 50–200 rpm, temperature varying from RT to 400 °C, time of 10–30 mins.

3 Results and Discussion

3.1 Effect of the Specimen Surface Treated by Different Methods on Sliding Friction Properties. The surface friction properties of T sample, S sample, SS sample, and TS sample were investigated on the condition of rotational speed of 200 rpm and load of 200 N with contact pressure of 0.92 MPa, as shown in Fig. 7. Examples of worn surface morphologies of the tested samples are shown in Fig. 8 by three-dimensional morphology analyzer. In this paper, the minimum sliding time is defined as the failure time when the friction coefficient reaches 0.7 in order to observably reflect the friction properties characterization of different samples.

As shown in Fig. 7, the friction coefficient of the four different samples from large to small is as follows: T sample, S sample, SS sample, and TS sample, and the failure time from large to small is as follows: TS sample, SS sample, S sample, and T sample. As shown in Fig. 7, the friction coefficient of T sample and S sample rapidly increase and end in failure with the increase of sliding time. TS sample and SS sample exhibit much longer failure time and much lower friction coefficient value than T sample and S sample. The friction coefficient of SS sample rapidly increases to about 0.4 in the starting period (0–66 s), and then remains relatively stable in the steady period (66–242 s), and afterward, rises to failure value (256 s).The friction coefficient of TS sample is the lowest, and remains relatively stable during the whole sliding process compared to that of the SS sample, T sample, and S sample.

As shown in Fig. 8, the surface wear of the S sample is the most serious, and obvious scratches appear on its surface along the sliding direction after wear, which shows that the serious adhesive wear appears on the S sample surface; the surface wear of the T sample, lighter than that of the S sample, occurs mainly around the microdimples, which illustrates that the textured surface without lubricant can slightly reduce the wear on the surface of sliding friction; the surface wear degree of the SS sample is lighter than that of the T sample and S sample, but still serious; the surface wear of the TS sample, with only a tiny wear trace and light abrasive wear, is the lightest abrasion compared to SS sample, T sample, and S sample.

Based on the above description, only the duplex treatment of processing microdimples and filling solid lubricant on the surface

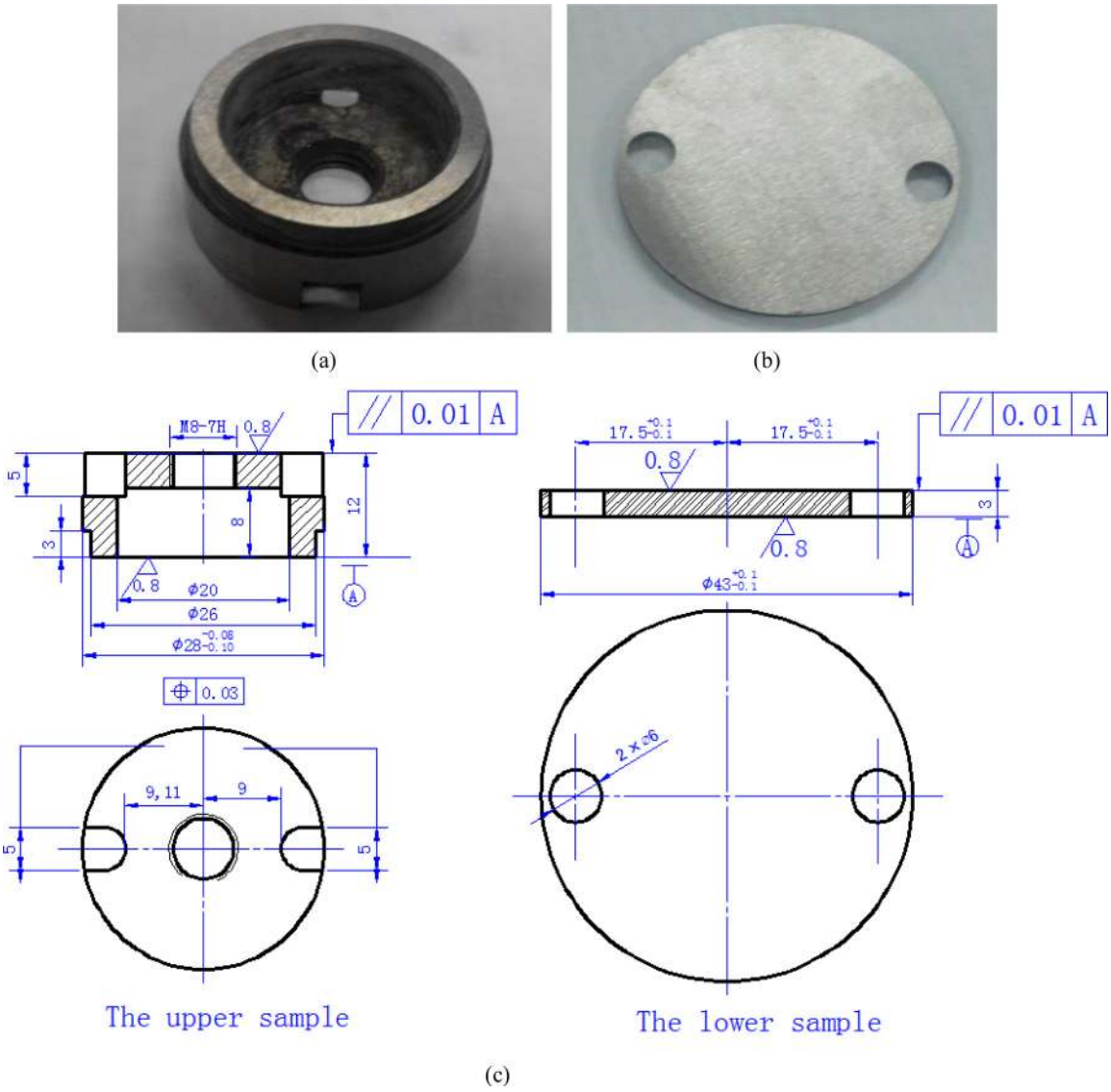

Fig. 1 The physical maps of the upper sample (*a*) and the lower sample (*b*) and the sample part drawing (*c*)

instead of the single treatment of machining microtexturing or smearing solid lubricant on the surface, can effectively improve the sliding friction performance of smooth surface, owing to the continuous layer of solid lubrication film. The textured surface without lubrication can reduce the wear of sliding friction surface in a certain extent due to the fact that the microdimples are able to trap wear particles. However, the textured surface without lubricant would increase the friction coefficient of the surface and shrink the lubrication failure time due to the large surface roughness of T sample in some range of the surface roughness. In addition, the smooth surface, coated with a layer of composite solid lubricant, could not effectively improve the sliding friction properties. A layer of solid lubricant film form between two sliding surfaces owing to the composite solid lubricant smeared on the specimen surface, which plays a certain role of lubrication. However, as the sliding continues, the solid lubricant between the smooth contact surfaces is gradually squeezed out of the friction pair, which results in the lack of effective supplement, and solid lubrication film on the surface is destroyed soon and loses the function of lubrication, which leads to the rapid increase of friction coefficient.

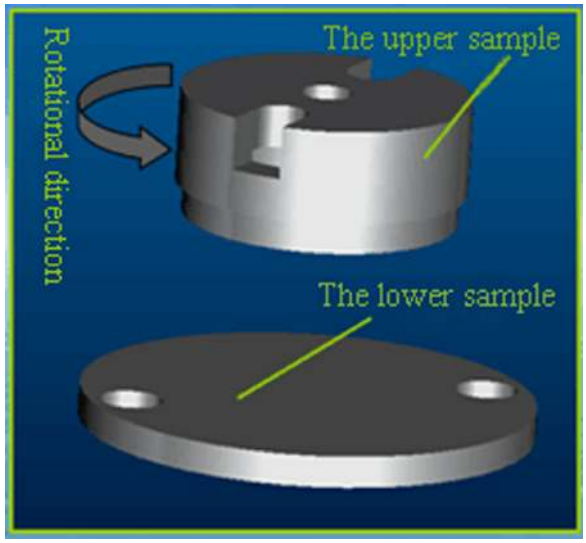

Fig. 2 Diagram of friction pair

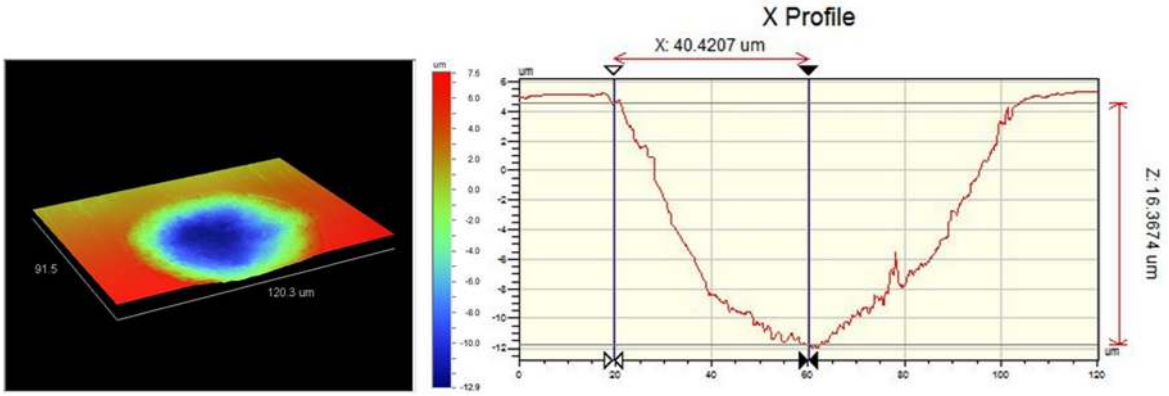

Fig. 3 The morphology of single microdimple of T sample with the texture density of 23% by a three-dimensional morphology analyzer

3.2 Effect of Texture Density on Sliding Friction Properties at Different Environment Temperatures. Test conditions are the rotational speed of 100 rpm, the test load of 100 N with contact pressure of 0.46 MPa, the test environment temperature of RT and high temperature of 200 °C and test time of 20 mins.

Figure 9 shows the curves of friction coefficients of the TS samples with the texture density of 12%, 23%, 35%, 46%, and 58% varied with time at RT and 200 °C, respectively. As shown in Fig. 9, at the beginning of the test, the friction coefficients of the samples rise rapidly to a maximum value first, and then remains relatively stable, reaching a process of "stable transition time." On the one hand, for most of metals, when put in the air, their surface would be almost immediately oxidized because the atom of the metal surface, usually in an imbalanced state, is easy to act with the surrounding medium to form a surface film that reduces the effect of surface molecular force by replacing the atomic bonding force or ion binding force between the friction pair with van der waals interaction, thus reducing the surface molecular force. In addition, shear force is small when it is sliding because the mechanical strength of the surface film is lower than that of the base material, and the friction surface is not easy to stick on account of the surface film, so the friction coefficient becomes small. On the other hand, before the start of the friction and wear test, the textured samples smeared with solid lubricating are placed for a long time and then act with environmental media to form a thin layer surface film in advance. In the initial stage of test, due to some lubrication function of this film, the friction coefficient is low, but increases rapidly and remains stable with the continuation of the experiment because the surface film is worn rapidly and a continuous and stable solid lubrication film appears gradually.

The variations of friction coefficient of the TS samples surface obtained by taking the average value in the stable period (180–1200 s) with the texture density at different temperatures are shown in Fig. 10. The friction coefficient of the TS sample decreases before increasing with the increase in the texture density, and the TS sample surface has the lower friction coefficient with texture density of 35% and 46% compared to that with texture density of 12%, 23%, and 58% at RT and 200 °C, respectively. Figure 11 shows the surface roughness of the TS sample varied with the texture densities of the lower samples after wear. It can be depicted that the surface roughness parameters of the upper sample decrease before increasing with the increase in the texture density of the lower sample. The surface roughness and the wear of the corresponding upper sample after wear are both the lightest with TS sample texture density of 46% compared to those with the TS sample texture density of 12%, 23%, 35%, and 58%. This is because the solid lubricant powder stored in dimples

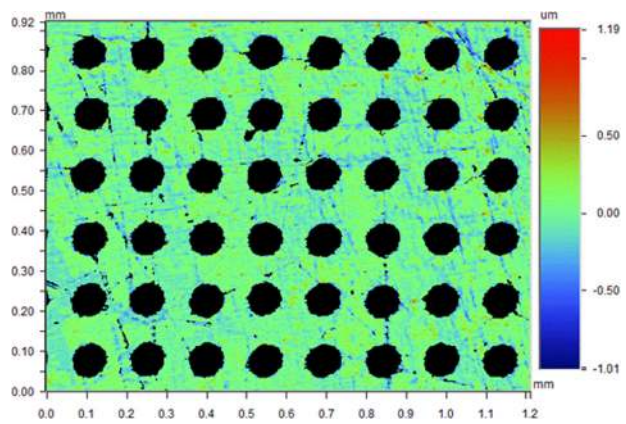

Fig. 4 The morphology of microtextured surface of T sample with the texture density of 23% by a three-dimensional morphology analyzer

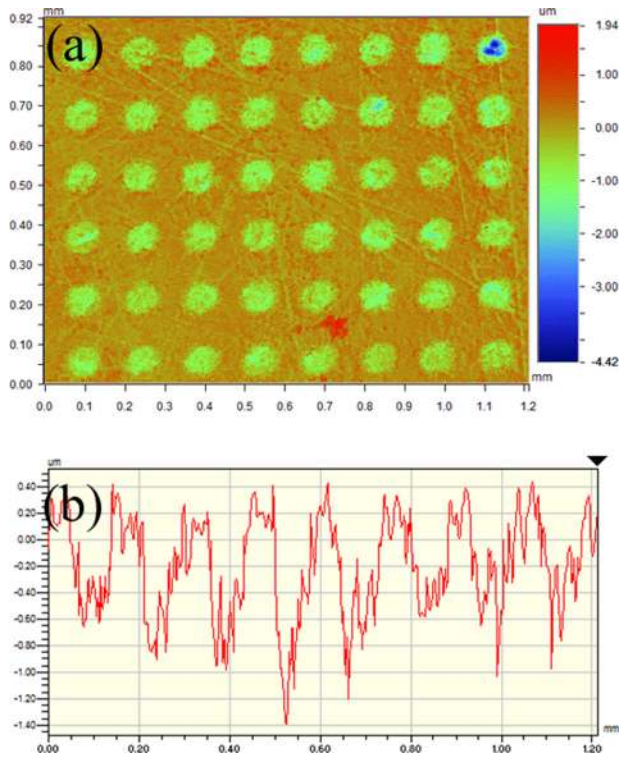

Fig. 5 The morphology (*a*) and the profile (*b*) of the T sample surface with the texture density of 23% filled with composite solid lubricant by three-dimensional morphology analyzer

Fig. 6 The figures of the MMU-10G high temperature friction and wear testing machine (*a*) and the test rig (*b*)

gets more with the increase in the texture density and then provides more benefits in repairing the damaged lubrication film on the sliding surface. In the meantime, the friction coefficient and the surface wear decrease, whereas too large texture density increases the surface roughness and the actual bearing area of the specimen surface, which results in the increase of the friction coefficient and wear volume.

3.3 Effect of Micron-Sized Solid Lubricant on Surface High Temperature Friction Properties

3.3.1 Effect of Environment Temperature on Sliding Friction Properties. Figure 12 shows the variations of friction coefficient of TS-1 sample in relation to temperature. It can be seen that the friction coefficient of TS-1 sample decreases before increasing with the increase in the temperature and it is lower at higher temperature than that at RT, but it is relatively small (about 0.1) in the temperature range of RT to 300 °C. Air humidity has some effect on the sliding friction performance of MoS_2. The lubrication effect of MoS_2 is better due to the smaller air humidity with the increase in the temperature. The friction coefficient of the TS-1 sample rapidly increases to about 0.44 when the environment temperature is up to 400 °C. The highest useful temperature of the adhesive film of the type of PI and MoS_2 is 380 °C and 370 °C, respectively. Thus, above 370 °C, MoS_2 is rapidly oxidized to MoS_3, and is slowly oxidized to MoO_3 with lubrication worse than that of MoS_2 at the temperature of 400 °C. In addition, the sliding friction itself would generate a lot of heat so that the friction surface temperature increases, leading to the friction surface temperature higher than 400 °C when the environment temperature is up to 400 °C. On the one hand, the softening and oxidation of the PI reduce the bearing capacity of the solid lubricant film, which makes the lubricating film prone to be destroyed. On the other hand, MoS_2 has been oxidized and its lubrication fails, which rapidly increases the friction coefficient. Figure 13

Table 1 The whole samples and the tested cases

Sample number	Surface treated by different methods
T	Textured surface without solid lubrication
S	Smooth surface without lubrication
SS	Smooth surface burnished with a layer of composite solid lubricant
TS	Textured surface filled with composite solid lubricant
TS-1	Textured surface filled with 20 wt.% PI + 80 wt.% micron-MoS_2
TS-2	Textured surface filled with 20 wt.% PI + 80 wt.% nano-MoS_2
TS-3	Textured surface filled with 20 wt.% PI + 74 wt.% nano-MoS_2 + 6 wt.% CNTs

Note: The texture density of TS-1sample, TS-2 sample, and TS-3 sample is 35%.

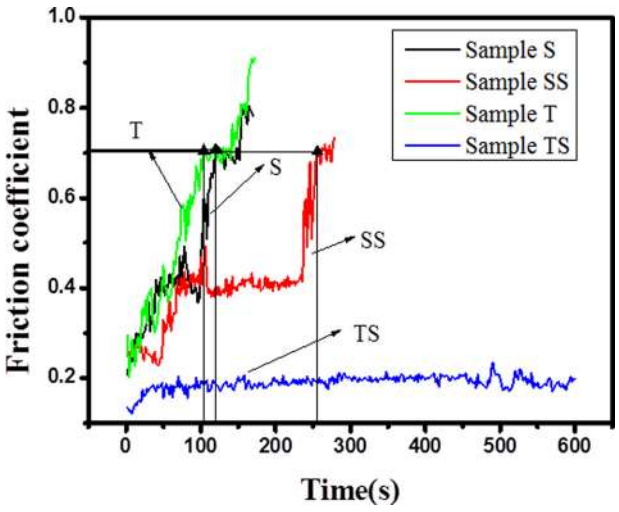

Fig. 7 The friction coefficient of T sample, S sample, SS samples, and TS sample varied with time (contact pressure of 0.92 MPa, rotational speed 200 r/min)

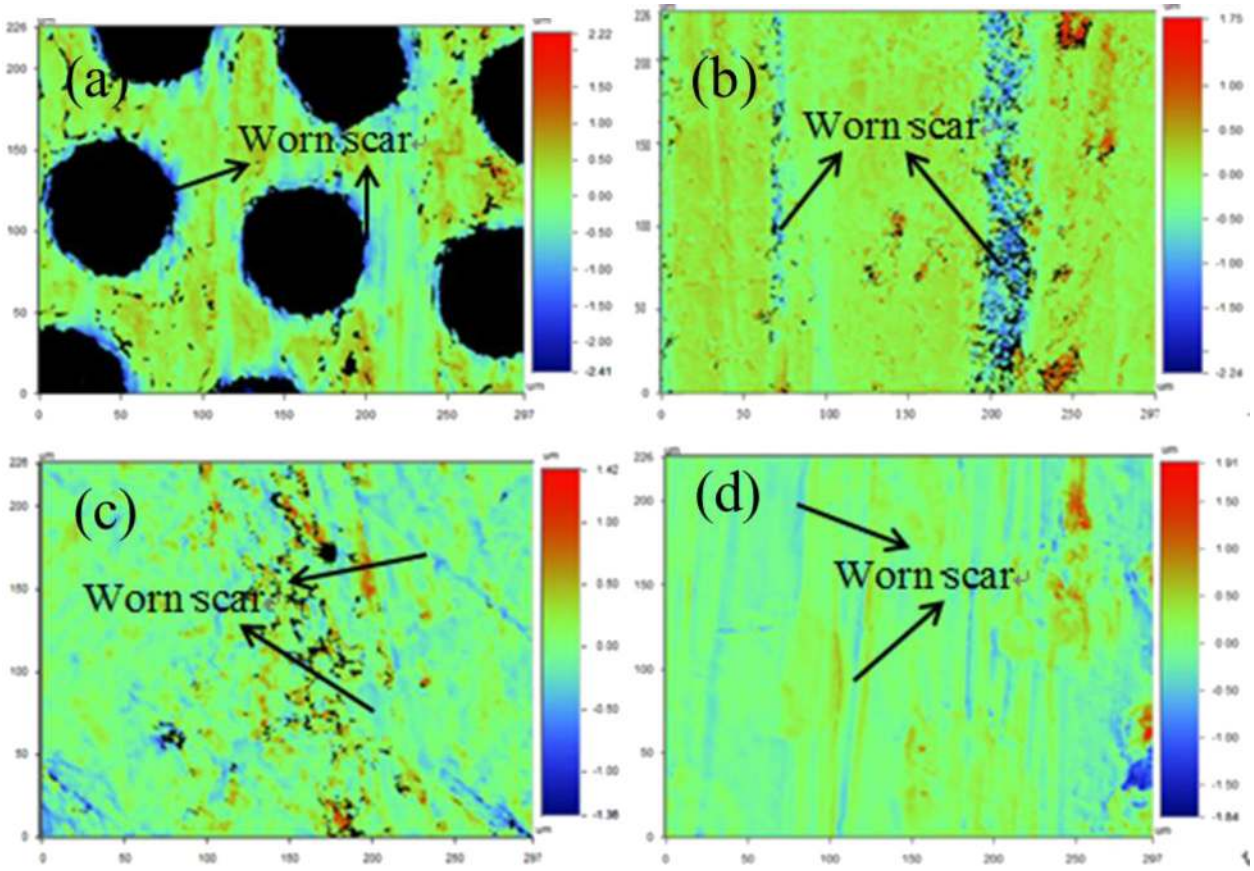

Fig. 8 Worn morphology of T sample (*a*), S sample (*b*), SS sample (*c*), and TS sample (*d*) after the wear test by a three-dimensional morphology analyzer

shows the XRD patterns of the TS-1 sample surface at different temperatures. The diffraction peaks in the XRD diagram correspond to MoS_2 peaks from RT to 300 °C, whereas it shows not only the emergence of the diffraction peaks corresponding to MoS_2 but also the appearance of the diffraction peak corresponding to MoO_3 at the environment temperature of 400 °C. It indicates that when the environment temperature is 400 °C, a part of the MoS_2 reacts with oxygen in the air at high temperature and generates MoO_3 with poorer lubricating performance.

3.3.2 Effect of Rotational Speed on the Friction Coefficient. Figure 14 shows the curves of the friction coefficients of the TS-1 sample varied with the rotational speed at different environment temperatures. The friction coefficient decreases before increasing with the increase of rotational speed. When the speed increases, the transferred speed of the solid lubricant from the microdimples to the surface becomes faster, so that the damaged solid lubricating film between the microdimples can get repaired rapidly. MoS_2 and PI powder in the solid lubricant have better grain orientation

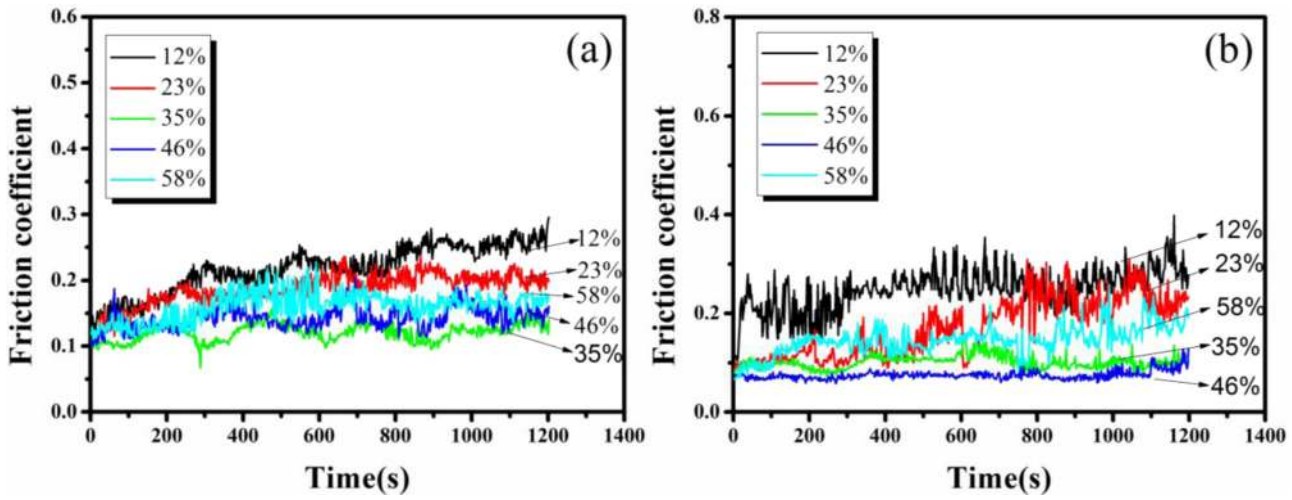

Fig. 9 The variation of friction coefficients of TS sample with the texture density of 12%, 23%, 35%, 46%, and 58% with sliding time at RT (*a*) and 200 °C (*b*) (contact pressure of 0.46 MPa, rotational speed 100 rpm)

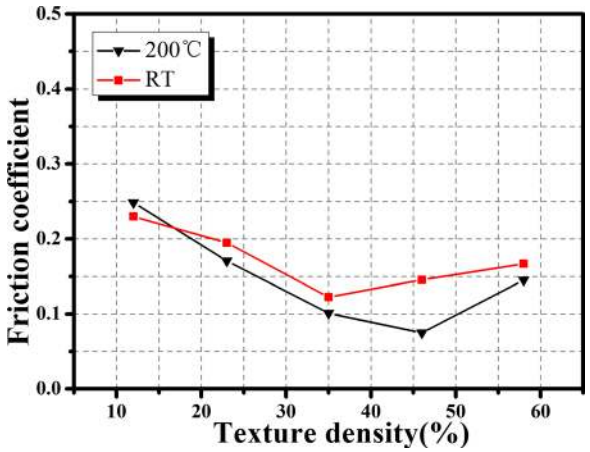

Fig. 10 The friction coefficient of TS sample versus dimple density at different temperatures (contact pressure of 0.46 MPa, rotational speed 100 rpm)

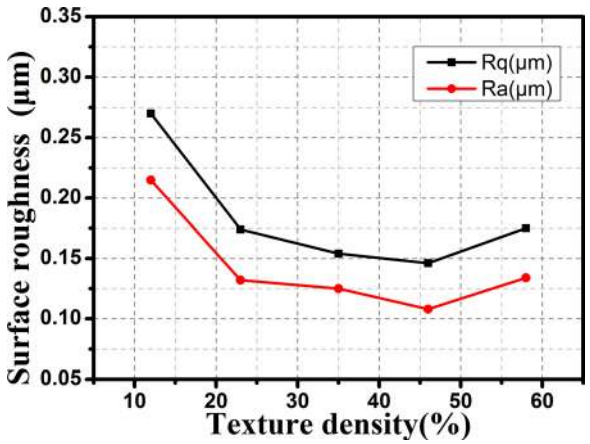

Fig. 11 The surface roughness of the upper sample versus dimple density of TS sample (contact pressure of 0.46 MPa, rotational speed 100 rpm)

due to high speed. And when the speed increases, the sliding friction generates more heat, which makes the PI component of solid lubricating material become softer and more prone to shear slip. Thus, the solid lubricant forms more easily a lubricating film in the sliding friction surface, playing a role of the better lubrication

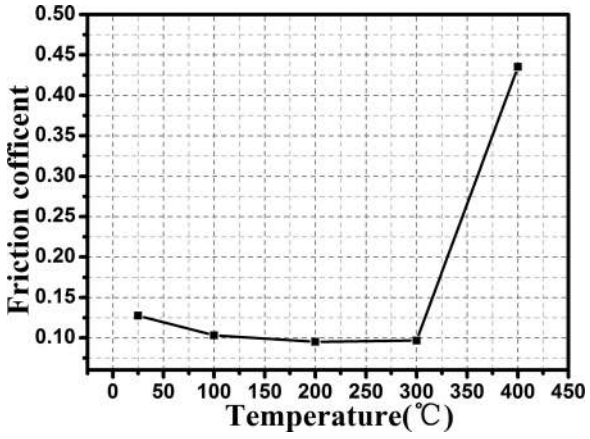

Fig. 12 The friction coefficient of TS-1 sample varied with temperature (contact pressure of 0.46 MPa, rotational speed 100 rpm, time 30 mins)

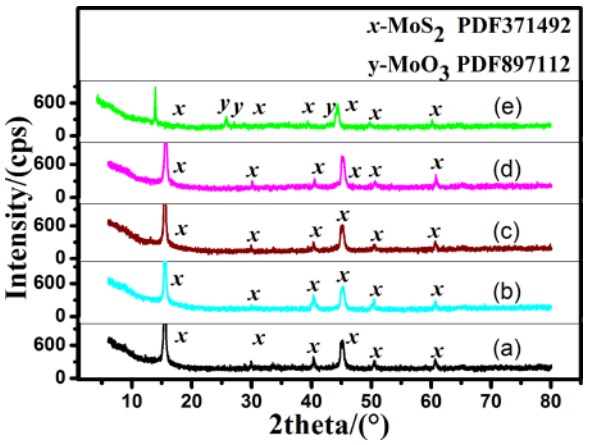

Fig. 13 XRD patterns of the surface of TS-1 sample at RT (*a*), 100 °C (*b*), 200 °C (*c*), 300 °C (*d*), and 400 °C (*e*)

antifriction effect. However, the friction coefficient of TS-1 sample decreases instead with further increase in the sliding speed. This is because when the speed is too high, the PI polymer chain has no time for orientation and is easy to break, resulting in debris and leading to wear [35], and MoS_2 bonded on PI has also become a part of wear debris, which damages the solid lubrication film and contributes to the increase in the friction coefficient.

3.3.3 Effect of Load on the Friction Coefficient. Figure 15 shows the curves of friction coefficient of the TS-1 sample surface under different loads at various environment temperatures. The friction coefficients of the TS-1 sample decreases with the increase in the load at the environment temperatures of RT and 100 °C. The larger load offers more benefits in squeezing more solid lubricant from the microdimples to the surface, thus forming the more compact solid lubrication film with better lubrication. Furthermore, when it is in the elastic plastic contact, the actual contact area of the contact surface is in nonlinear relationship with load, so that the friction coefficient decreases with the increase of the load. The friction coefficient of TS-1 sample decreases before increasing with the increase of the load at the environment temperature of 200 °C. The *pv* value of sliding friction surface increases accordingly when the load increases, and the friction of the sliding surface generates more heat and higher temperature softens the PI of solid lubrication and its mechanical performance becomes worse, so that the carrying capacity of solid lubrication film becomes worse; when bearing larger load, the PI is easier to be damaged, which worsens the continuity of the solid

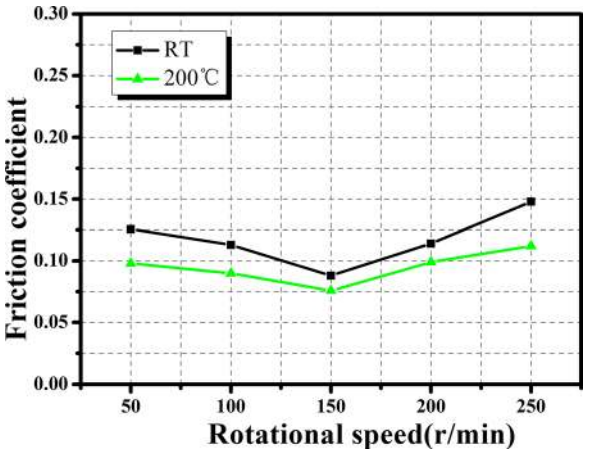

Fig. 14 The friction coefficient of sample TS-1 versus rotational speed (contact pressure: 0.46 MPa; time: 30 mins)

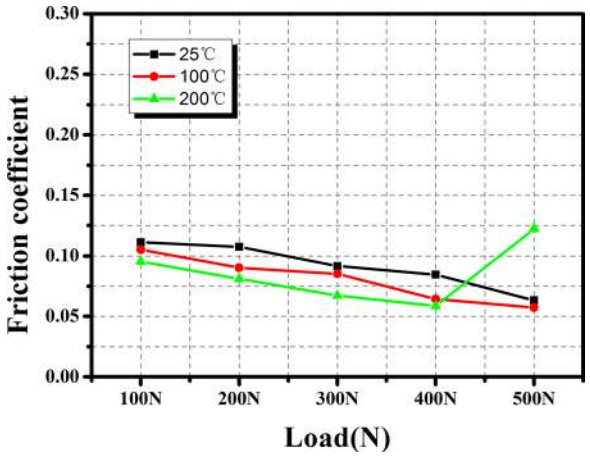

Fig. 15 The friction coefficient of sample TS-1 varied with load (rotate speed: 100 rpm; time: 30 mins)

lubricating film and reduces lubrication effect, thus contributing to the increase in the friction coefficient. However, the value of friction coefficient of the TS-1 sample sliding friction surface is still relatively low (about 0.12) and lubrication does not yield to failure, indicating the solid lubrication film still plays a better lubricating function. The friction coefficient of TS-1 sample increases under higher load compared to that under lower load, whereas it is still smaller compared to that of smooth surface without lubricant.

3.4 Effect of Nano-sized Solid Lubricant on Surface High Temperature Sliding Friction Properties

3.4.1 Effects of the Particle Size of Solid Lubricant Powder on the Friction Coefficient. Figure 16 shows the curves of friction coefficients of TS-1 sample, TS-2 sample and TS-3 sample varied with time. It can be seen that the friction coefficient of TS-2 sample is lower than that of TS-1 sample and the friction coefficient of TS-3 sample is lower than that of TS-2 sample. On one hand, the former comparison result indicates that the friction properties of microsurface texturing filled with nano-MoS_2 solid lubricant are better than those of micron-MoS_2. In other words, the lubrication performance of the nano-MoS_2 filled in microdimples is better than that of the micron-sized MoS_2. Nano-sized MoS_2 with the size smaller than that of common MoS_2 is more prone to be embedded into the friction pair surface wave and be reserved, thus increasing the actual contact area between the two sliding surfaces. Moreover, both the specific surface and the surface energy of nano-MoS_2 are larger than those of micron-sized MoS_2. In the cycled process, "extrusion-dispersion-formed film" (E-D-F) for the solid lubrication films on the surface, nano-sized MoS_2 with a high surface energy is more easily adsorbed on the surface of the friction pair, and thus accelerates the repaired effect of the worn solid lubricating film, which makes the solid lubrication film continuous and strong. Therefore, the lubricating effect of the textured surface filled with nano-MoS_2 solid lubricant is better than that of the micron-sized MoS_2. On the other hand, the latter friction coefficient comparison result of the TS-3 sample and the TS-2 sample demonstrates that the lubrication effect of the composite solid lubricant on the sample surface is improved due to the appropriate content of the CNTs. Due to the extreme high strength and extreme large toughness of CNTs, the strength and toughness of the composite solid lubrication film is improved. What's more, the good lubrication performance of the CNTs provides the benefits in the improvement of the lubricating properties of the composite solid lubrication.

3.4.2 Effect of Environment Temperature on Sliding Friction Properties of Nanocomposite Solid Lubricating Surface. The friction properties of MoS2-PI-CNTs composite solid lubricant containing 6 wt.% CNTs at temperatures ranging from RT to 400 °C were investigated on the condition of speed of 200 rpm and load of 200 N with a contact pressure of 0.92 MPa and the test time of each test was 30 mins.

Figure 17 shows curves of the friction coefficients of TS-3 samples varied with time at different temperatures. The friction coefficients of the TS-3 samples are relatively small in the temperature range of RT to 400 °C and TS-3 sample exhibits the lowest friction coefficient at 200 °C. The lubricant effect of MoS_2 is better with the smaller air humidity caused by the higher temperature, which makes the friction coefficient of the sample at 200 °C lower than that at the RT. MoS_2 evaporation rate would increase in the condition of high temperature above 430 °C because of the high temperature gradient of MoS_2 evaporation rate. Therefore, MoS_2 evaporation rate is relatively larger because the surface of the specimen might be far more than 430 °C ambient temperature due to friction heat. In addition, MoS_2 has been partially oxidized, so the lubricating effect of MoS_2 decreases, making the friction coefficient of TS-3 sample at 200 °C lower than that at 400 °C. Moreover, compared to Fig. 9, the results of Fig. 17 present that the friction coefficients of TS-3 samples are lower than those of the TS-1 sample at the temperature ranging from RT to 400 °C. Furthermore, the friction coefficients of the TS-3 sample remains still low at 400 °C, which illustrates that adding the appropriate mass

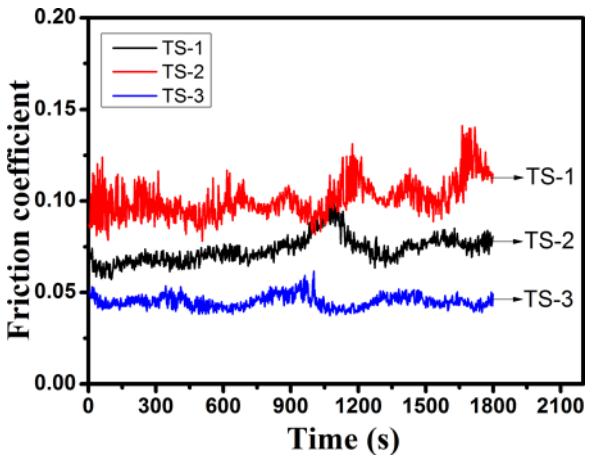

Fig. 16 Variations of the friction coefficient of TS-1 sample, TS-2 sample and TS-3 sample with the sliding time (contact pressure of 0.46 MPa, rotational speed 100 rpm, temperature 200 °C)

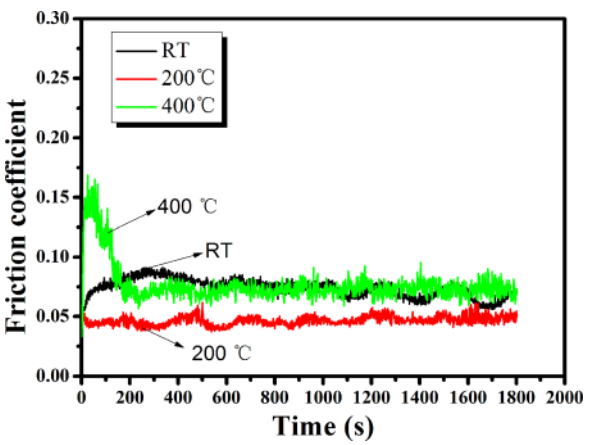

Fig. 17 Variations of the friction coefficient of TS-3 sample with the sliding time at different temperatures (contact pressure of 0.46 MPa, rotational speed 100 rpm)

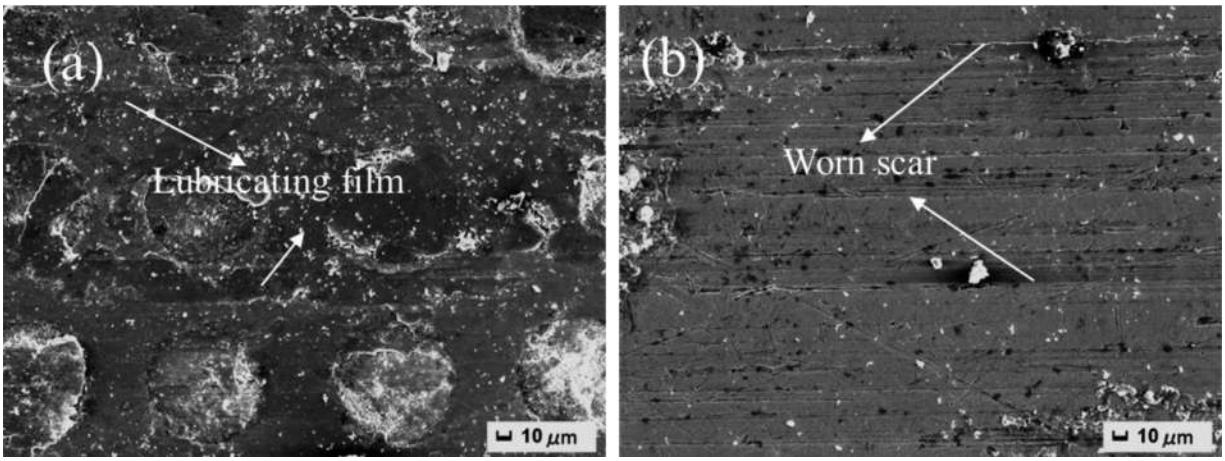

Fig. 18 The scanning electron microscopy (SEM) morphology of the surface of the sample TS (*a*) and the sample S (*b*) after the wear test

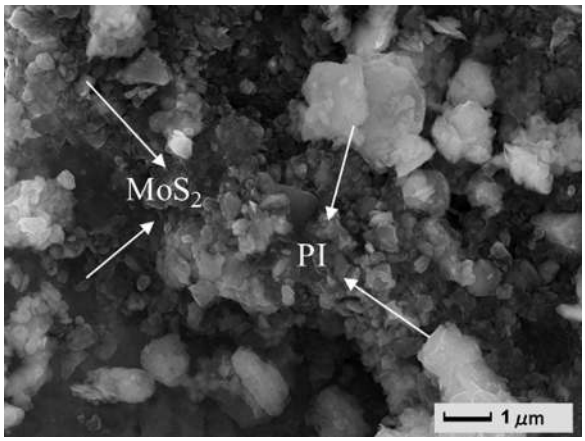

Fig. 19 The SEM topograph of MoS_2-PI composite solid lubrication

ratio of the CNTs in the MoS_2-PI composite solid lubricant can significantly improve the resistance high temperature sliding friction performance of the specimen. CNTs exhibit extremely high strength and extremely large toughness due to the fact that it consists of C-C covalent bond and the carbon atom distance and the diameter ingle-walled CNTs is small, which makes the solid lubrication film possess high strength and toughness and not be easily destroyed. In addition, tubular CNTs rolled on the lubricating surface, making the lubrication film of the specimen surface more uniform and compact. The composite lubricant formed by some chemical actions has better lubricating properties due to the fact that the CNTs themselves have good lubrication. The CNTs transmit thermal energy relying on ultrasonic in one-dimensional direction and its transmission speed is extremely high, reaching 10,000 m/s, so that the lubricant of the sample surface has an extreme high heat resistance. Therefore, the heat resistance and lubrication antifriction performance of MoS_2-PI-CNTs nano-sized composite solid lubricant are better than those of the MoS_2-PI composite lubricant.

3.5 Lubrication Mechanism Analysis. Figure 18 shows the worn surface morphologies of TS sample and S sample. When compared TS sample to S sample, the scratch morphology of the former is shallow and narrow, and that of the latter is deep and wide. There is a clear layer solid lubricating film on the TS sample surface compared to S sample surface. The two comparison results indicate that the combination technology of the solid lubricant and the LST can significantly reduce the abrasion of the sliding surface. The formation mechanism for the lubricating film is as follows: the thermal expansion coefficient of the selected solid lubricating material MoS_2-PI is higher than that of the metal matrix, so friction heat makes solid lubricating material MoS_2-PI

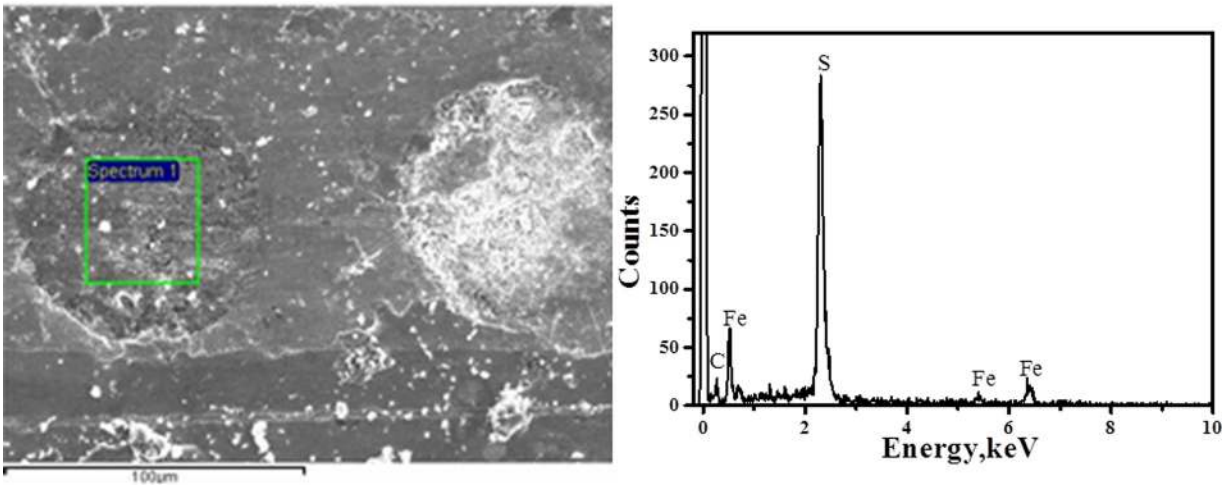

Fig. 20 EDS analysis on the microdimples of the TS sample after the wear test

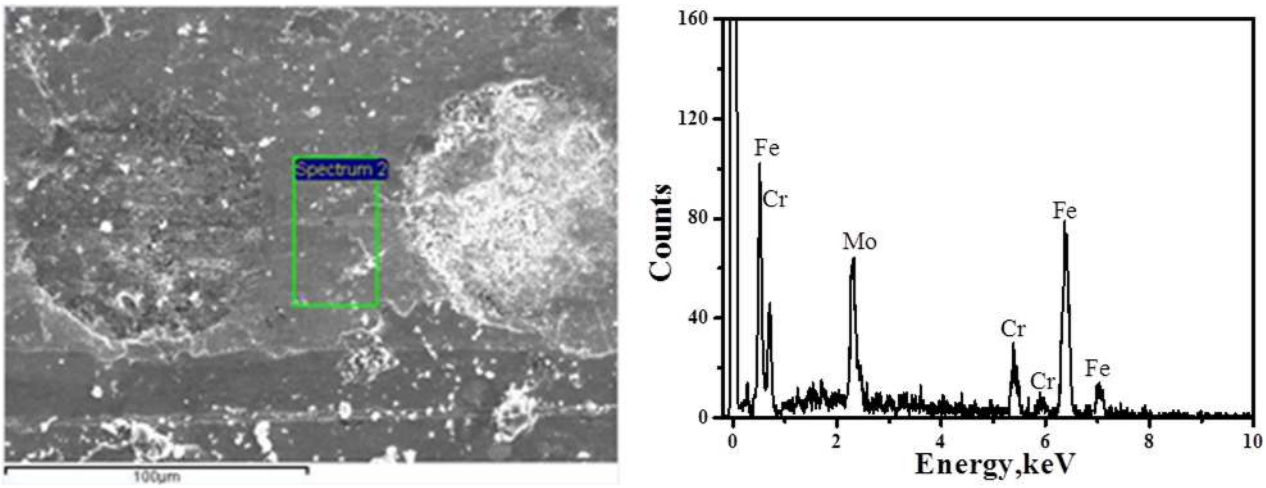

Fig. 21 EDS analysis on the surface between the microdimples of the TS sample after the wear test

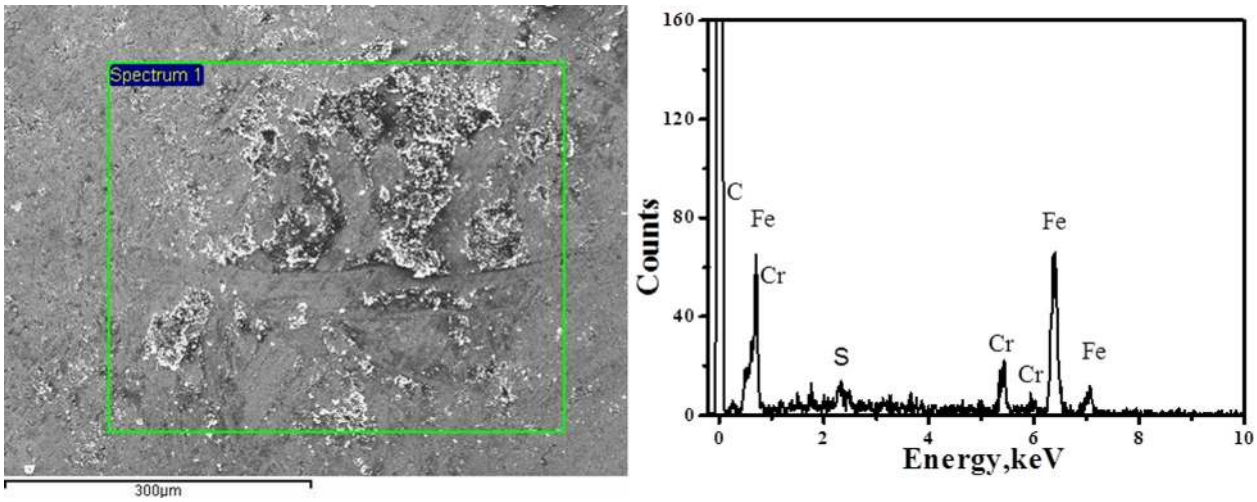

Fig. 22 EDS analysis on the surface of the upper sample after the wear test

expand and microprotrusions form on the sliding surface during the sliding process; a layer of solid lubrication film forms between and on the surface of the microdimples due to the fact that microprotrusion composite solid lubricating material produces shear slip when the two specimen surfaces are relatively sliding [36]. Figure 19 shows the micromorphology of the composite solid lubricant. It can be seen that the composite solid lubricant is comprised of the phases of MoS_2 and PI, and the flakelike large particle object is PI, playing the role of bond and the smaller particle object is MoS_2 dispersed in the PI particles or bonded on the surface of the flakelike large particles, functioning as the effect of lubrication.

Figure 20 shows the worn surface morphology of TS sample in the EDS elemental analysis in the dimples after wear. The presence of a small amount of iron makes it clear that the microdimple plays the role in a capturing abrasive. Figure 21 shows the worn surface of the TS sample in the EDS elemental analysis between the dimples after wear. There exist a large number of Mo elements between microdimples, indicating that the solid lubricant in the microdimples has transferred to the surface between the microdimples, and an effective solid lubricating film has formed on the surface. Figure 22 shows the EDS map of the upper sample pairing with TS sample. The appearance of S element indicates that the solid lubrication on the surface of lower sample has transferred to the surface of the upper sample. The direct contact between metal and metal has been changed to the indirect contact between the solid lubricating films due to the solid lubricating film on the surface of the TS sample and the transfer film on the surface of the upper sample.

Compared to the SS sample, the solid lubricant on the TS sample surface is not easy to be squeezed out of the friction pair due to the microdimples on the surface that can capture and store solid lubricant in the sliding process. And then the solid lubrication film forms again between the microdimples with the solid lubrication heated to expand because of the sliding friction. It cycles constantly as above that the worn solid lubricating film gets supplemented and repaired well, which makes the solid lubricating film on the textured surface continuous and stable. Thus the friction coefficient and the wear of specimen surface get reduced.

4 Conclusion

(1) The friction coefficient of the textured surface filled with composite lubricant (TS) retains the lowest value and the highest stability compared to textured surface without solid lubrication (T), smooth surface without lubrication (S), and smooth surface burnished with a layer of composite solid lubricant (SS).

(2) The friction coefficient of TS sample decreases before increasing with the increase of the dimple density, and the better dimple density range is 35–46%.
(3) The friction coefficients of the sample surface filled with micron-composite solid lubricant with the texture density of 35% (TS-1) are maintained at a low level in the environment temperature range of RT to 300 °C.
(4) The friction coefficient of TS-1 sample decreases before increasing with the increase of rotational speed.
(5) The friction coefficients of TS-1 sample decrease with the increase of the rotational speed at RT and 100 °C, and the friction coefficient decreases before increasing with the increase of the rotational speed at 200 °C.
(6) The lubrication performance of the nano-MoS_2 filled in micro-surface texturing is better than that of the micron-MoS_2.
(7) The friction coefficients of the samples filled with MoS_2-PI-CNTs nano-sized composite solid lubricant are all relatively small in the temperature range of RT to 400 °C and lower than those of the samples filled with the MoS_2-PI composite lubricant.

Acknowledgment

This research was supported by National Natural Science Foundation of China (Nos. 51375211, 51305168, and 51175233).

References

[1] Geiger, M., Roth, S., and Becker, W., 1998, "Influence of Laser-Produced Microstructures on the Tribological Behaviour of Ceramics," Surf. Coat. Technol., **100–101**, pp. 17–22.
[2] Etsion, I., 2005, "State of the Art in Laser Surface Texturing," ASME J. Tribol., **127**(1), pp. 248–253.
[3] Ji, J., Fu, Y., and Bi, Q., 2014, "Influence of Geometric Shapes on the Hydrodynamic Lubrication of a Partially Textured Slider With Micro-Grooves," ASME J. Tribol., **136**(4), pp. 216–223.
[4] Hong, D. D., Iwatani, N., and Fushinobu, K., 2013, "Laser Processing by Using Fluidic Laser Beam Shaper," Int. J. Heat Mass Transfer, **64**, pp. 263–268.
[5] Wang, X., and Kato, K., 2003, "Improving the Anti-Seizure Ability of SiC Seal in Water With RIE Texturing," Tribol. Lett., **14**(4), pp. 275–280.
[6] Zhang, J., and Meng, Y., 2012, "A Study of Surface Texturing of Carbon Steel by Photochemical Machining," J. Mater. Process. Technol., **212**(10), pp. 2133–2140.
[7] Ji, J., Fu, Y., Wei, L., Hua, X., and Bi, Q., 2011, "Experiment Research on Lubrication Properties of Laser Surface Texturing Mechanical Seal," J. Drain. Irrig. Mach. Eng., **29**(5), pp. 427–431.
[8] McNickle, A. D., and Etsion, I., 2004, "Near-Contact Laser Surface Textured Dry Gas Seals," ASME J. Tribol., **126**(4), pp. 788–794.
[9] Brizmer, V., Kligerman, Y., and Etsion, I., 2003, "A Laser Surface Textured Parallel Thrust Bearing," Tribol. Trans., **46**(3), pp. 397–403.
[10] Brizmer, V., and Kligerman, Y., 2012, "A Laser Surface Textured Journal Bearing," ASME J. Tribol., **134**(3), pp. 308–314.
[11] Gadeschi, G. B., Backhaus, K., and Knoll, G., 2012, "Numerical Analysis of Laser-Textured Piston-Rings in the Hydrodynamic Lubrication Regime," ASME J. Tribol., **134**(4), p. 041702.
[12] Mariani, G., 2009, *Lubricant Additives: Chemistry and Applications*, R. L. Rudnick, ed., CRC Press, Boca Raton, pp. 173–194.
[13] Segu, D. Z., Kim, J. H., Si, G. C., Jung, Y. S., and Kim, S. S., 2013, "Application of Taguchi Techniques to Study Friction and Wear Properties of MoS_2 Coatings Deposited on Laser Textured Surface," Surf. Coat. Technol., **232**, pp. 504–514.
[14] Ripoll, M. R., Brenner, J., and Podgornik, B., 2013, "Friction and Lifetime of Laser Surface–Textured and MoS_2-Coated Ti6Al4V Under Dry Reciprocating Sliding," Tribol. Lett., **51**(2), pp. 261–271.
[15] Tagawa, N., Andoh, H., and Tani, H., 2010, "Study on Lubricant Depletion Induced by Laser Heating in Thermally Assisted Magnetic Recording Systems: Effect of Lubricant Thickness," Tribol. Lett., **37**(2), pp. 411–418.
[16] Rapoport, L., Moshkovich, A., Perfilyev, V., Lapsker, I., Halperin, G., Itovich, G., and Etsion, I., 2008, "Friction and Wear of MoS2 Films on Laser Textured Steel Surfaces," Surface Coat. Technol., **202**(14), pp. 3334–3340.
[17] Wu, Z., Deng, J., Zhang, H., Yun, S., and Zhao, J., 2012, "Tribological Behavior of Textured Cemented Carbide Filled With Solid Lubricants in Dry Sliding With Titanium Alloys," Wear, **292–293**, pp. 135–143.
[18] Rapoport, L., Moshkovich, A., Perfilyev, V., Gedanken, A., Koltypin, Y., Sominski, E., Sominski, G., and Etsion, I., 2009, "Wear Life and Adhesion of Solid Lubricant Films on Laser-Textured Steel Surfaces," Wear, **267**(5), pp. 1203–1207.
[19] Hu, T., Zhang, Y., and Hu, L., 2012, "Tribological Investigation of MoS_2 Coatings Deposited on the Laser Textured Surface," Wear, **278–279**, pp. 77–82.
[20] Li, J., Xiong, D., Huang, Z., Kong, J., and Dai, J., 2009, "Effect of Ag and CeO_2 on Friction and Wear Properties of Ni-Base Composite at High Temperature," Wear, **267**(1), pp. 576–584.
[21] Murakami, T., Ouyang, J. H., Sasaki, S., Umeda, K., and Yoneyama, Y., 2007, "High-Temperature Tribological Properties of Spark-Plasma-Sintered Al_2O_3 Composites Containing Barite-Type Structure Sulfates," Tribol. Int., **40**(2), pp. 246–253.
[22] Aouadi, S. M., Luster, B., Kohli, P., Muratore, C., and Voevodin, A. A., 2009, "Progress in the Development of Adaptive Nitride-Based Coatings for High Temperature Tribological Applications," Surf. Coat. Technol., **204**(6), pp. 962–968.
[23] Li, J., Xiong, D., Zhang, Y., Zhu, H., Qin, Y., and Kong, J., 2011, "Friction and Wear Properties of MoS_2-Overcoated Laser Surface-Textured Silver-Containing Nickel-Based Alloy at Elevated Temperatures," Tribol. Lett., **43**(2), pp. 221–228.
[24] Li, J., Xiong, D., Wu, H., Zhang, Y., and Qin, Y., 2013, "Tribological Properties of Laser Surface Texturing and Molybdenizing Duplex-Treated Stainless Steel at Elevated Temperatures," Surf. Coat. Technol., **228**(Suppl. 1), pp. S219–S223.
[25] Oksanen, J., Hakala, T. J., Tervakangas, S., Laakso, P., Kilpi, L., Ronkainen, H., and Koskinen, J., 2014, "Tribological Properties of Laser-Textured and ta-C Coated Surfaces With Burnished WS_2 at Elevated Temperatures," Tribol. Int., **70**, pp. 94–103.
[26] Wang, Y., Zhou, H., Chen, J., Chen, L., and Ye, Y., 2010, "Preparation and Friction and Wear Behavior of Waterbome Epoxy Resin-Based Bonded Solid Lubricant Coatings," Tribology, **30**(6), pp. 577–583.
[27] Luo, J., Wang, Y., Cai, Z., Mo, J., Peng, J., and Zhu, M., 2012, "Rotational Fretting Wear Characteristics of Bonded MoS_2 Solid Lubrication Coating," J. Mech. Eng., **48**(17), pp. 100–105.
[28] Chen, J., Zuo, H., Fan, L., and Yang, S., 2006, "Development of High Temperature Polyimide," Aerosp. Mater. Technol., **36**(2), pp. 7–12.
[29] Zhu, P., Wang, X. D., Huang, P., Wang, X., and Shi, J., 2005, "Tribology Performance of Molybdenum Disulfide Reinforced Thermoplastic Polyimide," Tribology, **25**(5), pp. 441–445.
[30] Wang, T., Shao, X., Wang, Q., and Liu, W., 2005, "Preparation and Research on the Friction and Wear Properties of Polyimide/Molybdenum Disulfide Intercalation Composite Material," Tribology, **25**(4), pp. 322–327.
[31] Xu, J., Zhu, M., Liu, H., Chen, J., and Zhou, Z., 2004, "Influence of Relative Humidity, Temperature, Oil Lubricantion on the Fretting Wear Life of Bonded Solid Lubricant Coating," Mater. Mech. Eng., **27**(9), pp. 21–23.
[32] Chen, W., Li, F., Han, G., Xia, J., Wang, L., and Tu, J., 2003, "Tribological Behavior of Carbon-Nanotube-Filled PTFE Composites," Tribol. Lett., **15**(3), pp. 275–278.
[33] Li, S., Feng, Y., and Yang, X., 2010, "Influence of Adding Carbon Nanotubes and Graphite to Ag-MoS_2 Composites on the Electrical Sliding Wear Properties," Acta Metall. Sin. (Engl. Lett.), **23**(1), pp. 27–34.
[34] Altavilla, C., Sarno, M., Ciambelli, P., Senatore, A., and Petrone, V., 2013, "New 'Chimie Douce' Approach to the Synthesis of Hybrid Nanosheets of MoS_2 on CNT and Their Anti-Friction and Anti-Wear Properties," Nanotechnology, **24**(12), p. 125601.
[35] Chong, P., Li, T., and Zhang, X., 1998, "Advancing in Tribological Characteristics Research of Polyimide Solid-Lubricating Films," Mater. Sci. Eng., **16**(1), pp. 50–52.
[36] Huang, G., and Liu, Z., 2008, "The Inlaid Solid Lubricating Material Design," J. Liaoning Inst. Sci. Technol., **10**(2), pp. 14–15.